Carbohydrate Polymers 116 (2015) 261–266

Contents lists available at ScienceDirect

Carbohydrate Polymers

journal homepage: www.elsevier.com/locate/carbpol

Photoreductive generation of amorphous bismuth nanoparticles using polysaccharides – Bismuth–cellulose nanocomposites

Doris Breitwieser[a], Margit Kriechbaum[b], Heike M.A. Ehmann[a], Uwe Monkowius[b], Sergiu Coseri[c], Liviu Sacarescu[c,**], Stefan Spirk[d,e,*]

[a] Institute for Chemistry, University of Graz, Heinrichstrasse 24, 8010 Graz, Austria
[b] Johannes-Kepler-University Linz, Institute of Inorganic Chemistry, Altenbergerstraße 69, 4040 Linz, Austria
[c] "Petru Poni" Institute of Macromolecular Chemistry, Aleea Grigore Ghica Voda 41A, 700487 Iasi, Romania
[d] Graz University of Technology, Institute for Chemistry and Technology of Materials, Stremayrgasse 9, 8010 Graz, Austria
[e] University of Maribor, Institute for the Engineering and Design of Materials, Smetanova Ulica 17, 2000 Maribor, Slovenia

ARTICLE INFO

Article history:
Received 4 December 2013
Received in revised form 9 May 2014
Accepted 10 June 2014
Available online 16 June 2014

Keywords:
Cellulose
Trimethylsilyl cellulose
Bismuth nanoparticles
Photoreduction
Photochemistry

ABSTRACT

A simple and highly reproducible synthesis of amorphous bismuth nanoparticles incorporated into a polysaccharide matrix using a photoreduction process is presented. As precursor for the generation of the Bi nanoparticles, organosoluble triphenylbismuth is used. The precursor is dissolved in toluene and mixed with a hydrophobic organosoluble polysaccharide, namely trimethylsilyl cellulose (TMSC) with high DS_{Si}. The solution is subjected to UV exposure, which induces the homolytic cleavage of the bismuth–carbon bond in $BiPh_3$ resulting in the formation of Bi^0 and phenyl radicals. The aggregation of the Bi atoms can be controlled in the TMSC matrix and yields nanoparticles of around 20 nm size as proven by TEM. The phenyl radicals undergo recombination to form small organic molecules like benzene and biphenyl, which can be removed from the nanocomposite after lyophilization and exposure to high vacuum. Finally, the TMSC matrix is converted to cellulose after exposure to HCl vapors, which remove the trimethylsilyl groups from the TMSC derivative. Although TMSC is converted to cellulose, the formed TMS-OH is not leaving the nanocomposite but reacts instead with surface oxide layer of the Bi nanoparticles to form silylated Bi nanoparticles as proven by TEM/EDX.

1. Introduction

Bulk bismuth features a set of properties, which are highly demanded in many areas of materials sciences. It plays a major role in the design of new semiconductors (large Fermi wavelengths (Smith, Baraff, & Rowell, 1964), strong diamagnetism, very high magneto-resistance) (Murakami, 2006), as well as in medicine, where the rather low human toxicity of several bismuth compounds is exploited to treat different kind of illnesses (Briand & Burford, 1999). A well known example is its action against *Helicobacter pylori*, a bacterium associated with the pathogenesis of gastroduodenal ulcers (Tsang, Ho, Sun, & Chan, 2011). Further applications in medicine include the use of bismuth (and its compounds) as contrast agents owing to its large scattering contrast (Lusic & Grinstaff, 2013; Yu & Watson, 1999). On the other hand, bismuth nanoparticles (BiNPs) have been explored to a much less extent than bulk bismuth. This can be related to difficulties in producing nanoparticles with a defined size and shape. Up to date the most convenient synthesis of BiNPs includes the reduction of organometallic precursors (*e.g.* $Bi(NTMS_2)_3$) which can be stabilized using synthetic polymers (Wang, Tang, Yu, Gibbons, & Buhro, 2008). Through this approach, the size and the shape of the nanoparticles can be efficiently controlled and size dependent electronic properties can be further investigated (Yarema, Kovalenko, Hesser, Talapin, & Heiss, 2011). However, one major drawback of this strategy is the use of synthetic polymers, which limits the applicability of such systems. It would be highly desirable to employ biodegradable and biocompatible polymers such as polysaccharides for this purpose. In addition, the Bi-precursors are not readily available and must be synthesized prior to nanoparticle preparation (Lutz et al., 2012; Reith, Stiftinger, Monkowius, Knoer, & Schoefberger, 2011; Imran et al., 2013). An alternative

* Corresponding author at: Graz University of Technology, Institute for Chemistry and Technology of Materials, Stremayrgasse 9, 8010 Graz, Austria.
Tel.: +43 316 873 32284.
** Corresponding author.
E-mail addresses: livius@icmpp.ro (L. Sacarescu), stefan.spirk@tugraz.at (S. Spirk).

http://dx.doi.org/10.1016/j.carbpol.2014.06.017
0144-8617/

is to use a photoreduction process for the generation of nanoparticles (Warren, Jackson, Cater-Cyker, DiSalvo, & Wiesner, 2007). In the course of photoreduction, photolabile Bi-element bonds are homolytically cleaved (Fischereder et al., 2013) and elemental bismuth is obtained. An excellent precursor for this purpose is triphenyl bismuth, which is cheap, readily available, non-toxic, and, most importantly, which offers photolabile Bi-carbon bonds. Moreover, $BiPh_3$ is highly soluble in several organic solvents such as toluene and exhibits thermal stability in the absence of oxygen (*ca.* 200°) (Berger et al., 2012). The interesting properties of bismuth (nanoparticles) inspired us to incorporate this element in cellulosic matrices. Problems to be addressed involve the photochemical stability of the chosen solvent/polysaccharide and to identify polysaccharide derivatives that feature a similar solubility like $BiPh_3$. In addition, the polysaccharide polarity should be tuneable in terms of hydrophilicity/hydrophobicity in order to enable a variety of applications (*e.g.* in textiles and medicine). An elegant way to achieve such a tuneable hydrophilicity/hydrophobicity is the use of polysaccharides bearing acid or alkaline labile groups. While the removal of acetate groups in organosoluble cellulose acetate requires strong bases for instance, the use of acid labile silyl ethers of polysaccharides can be easily performed with acidic vapors of HCl. In this paper, we present an approach how to tackle these problems by using trimethylsilyl cellulose with high DS_{Si} in the course of a photoreduction process of $BiPh_3$. The solubility of trimethylsilyl cellulose (TMSC) is strongly dependent on the DS_{Si} and ranges from ethanol (DS ~0.7), DMSO (~1.5) to chloroform and toluene (>2.5). Chloroform is not photochemically stable upon UV exposure (forms $Cl^{\bullet}$) therefore toluene seems to be the appropriate choice. In addition, the use of TMSC provides an elegant way to convert a hydrophobic matrix (for high DS_{Si}) into a hydrophilic one. Although other biodegradable and biocompatible polymers could be used for such a purpose as well (*i.e.* by silylation and subsequent desilylation) the use of polysaccharide derivatives provides much more potential applications due the rather high range of molar masses available, the rather good photochemical stability of many polysaccharides at $\lambda > 300$ nm and the compatibility with other biobased materials such as cellulose fibers, films and papers. This compatibility is a crucial point since it allows to coat or impregnate these materials easily. Although we do not investigate enzymatic digestability of the polysaccharide matrix in this paper, it could be relevant for a variety of applications particularly in case free bismuth nanoparticles are desired.

2. Materials and methods

2.1. Materials

Trimethylsilyl cellulose (TMSC) with a DS_{Si} value of 2.55 (M_w = 175,000, M_n = 36,000, kindly provided by the Centre of Excellence for Polysaccharide Research, University of Jena) was used for nanoparticle stabilization. Toluene (99.9%) was purchased from Sigma–Aldrich and $BiPh_3$ (95%) was obtained from ABCR, Germany.

2.2. Preparation of monodisperse bismuth nanoparticles

In a typical experiment, a toluene solution containing $BiPh_3$ (5 wt.%) and TMSC (1 wt.%) was irradiated with a HBO lamp 100W/2 under stirring in a sealed quartz glass test tube for 2 h under N_2 atmosphere. The formation of nanoparticles is accompanied with a brownish coloration of the solution. Afterwards, the particles are lyophilized and exposed to vacuum conditions for a period of 3 h at room temperature in order to remove the byproduct biphenyl.

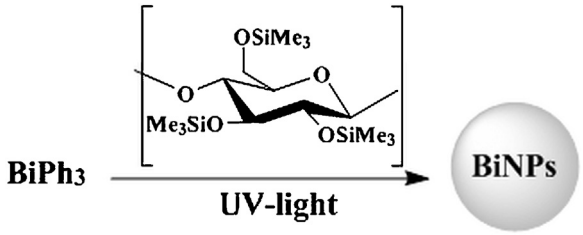

Fig. 1. Schematic overview on photoreduction of $BiPh_3$ using trimethylsilyl cellulose. For reasons of clarity, all hydroxy groups are substituted by silyl groups; the actual DS_{Si} is 2.55.

2.3. Characterization of BiNPs

The studies of size, morphology and composition of the nanoparticles were performed by means of transmission electron microscopy (TEM) and energy dispersive X-ray using a HITACHI HT7700 microscope equipped with a Bruker XFlash 6 EDS detector operated at 120 kV in high contrast mode. The samples for TEM analysis have been prepared by placing small droplets of a diluted (by ~100 × with toluene) dispersions (1 wt.%) on copper grids (300 mesh) coated with an amorphous carbon film (Ted Pella, Redding, CA) and dried at 50 °C in vacuum for 24 h prior to the measurements.

3. Results and discussion

In first trials, the generation of bismuth particles starting from toluene solutions of $BiPh_3$ without stabilizers was investigated. Even after a few minutes of UV exposure, a massive gray precipitate was observed in the solution (data not shown). This indicates a rather fast aggregation of the nanoparticles after formation of elemental bismuth, which is often observed for photoreduction processes. In general, a common strategy to control the growth of nanoparticles is to add polymers, which act as steric stabilizers preventing uncontrolled aggregation of NPs by interaction with the nanoparticle surface. However, there are several constraints on the choice of the polymeric stabilizer. It should be compatible with the solubility of the precursor (*i.e.* toluene), it should exhibit sufficient photochemical stability under the chosen conditions, it should be tunable in terms of hydrophilicity/hydrophobicity while being biodegradable/biocompatible to ensure a wide range of applications. Keeping these facts in mind, a few polymers come into the closer choice such as cellulose acetates (CA) and silylethers of cellulose. These show excellent solubility at high DS in organic solvents such as toluene and can be converted to cellulose by simple procedures (*e.g.* either by aqueous alkali treatment for CA or exposure to HCl vapor for TMSC). The use of an aqueous conversion procedure imposes the risk that the formed nanoparticles are altered by this step; therefore TMSC (Koehler, Liebert, & Heinze, 2008) was chosen as the hydrophobic polysaccharide stabilizer for Bi-NPs in order to demonstrate the proof of principle (Fig. 1)

Moreover, TMSC at high DS_{Si} is soluble in toluene and exhibits sufficient photostability under the chosen reaction conditions. The DS_{Si} of the TMSC remains stable during the irradiation, since TMSC derivatives with lower DS values would be insoluble in toluene resulting in the formation of a precipitate. However, we did not observe any precipitates during our synthesis procedures. When irradiating TMSC solutions in the absence of $BiPh_3$ under nitrogen atmosphere for 1 h, we could not detect a major decrease in the DP as proven by GPC (data not shown).

In a typical procedure, TMSC is added to solutions containing $BiPh_3$ and clear, colorless solutions with low viscosity are obtained. After exposure to polychromatic UV-light, BiNPs are formed within 2 h which can be followed by a slightly browning of the solution.

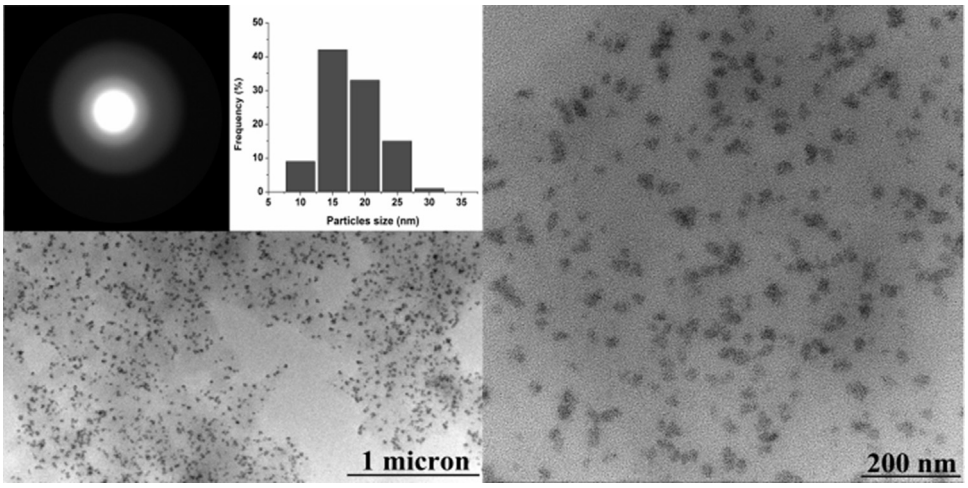

Fig. 2. TEM images of BiNPs generated by photoreduction of $BiPh_3$ in the presence of trimethylsilyl cellulose in different magnifications. The scattering pattern of the particles is shown in the upper left corner.

In general, the strength of metal–carbon bonds of main group metals considerably decreases with increasing atomic number (Elschenbroich, 2005). Hence, it is not surprising that these bonds are prone to photo-cleavage. The photo-decomposition of several compounds with s^2 configuration has been investigated in the past (Tl^+, Pb^{2+}, Bi^{3+}, etc. (Kunkely, Paukner, & Vogler, 1989; Oldenburg, Vogler, Mikó, & Horváth, 1996; Vogler & Nikol, 1992)), among them also Ph_3Bi (Paez & Hoggard, 2003). Frequently, these compounds form elemental metal and oxidation products upon irradiation. The oxidation products result from a coupling of the ligands or from the reaction of a possibly formed radical with the solvent. The mechanism is strongly dependent on the reaction conditions as well as the ligand or organic groups bonded to the bismuth atom and not always clear. Two reactive excited states or a mixture thereof are usually discussed to be responsible for the photo-decomposition, namely a metal centered sp- and a ligand-to-metal charge transfer (LMCT) transition. In both cases the photo-excitation leads to the same LUMO, *i.e.* to an antibonding σ^* orbital, whereas the HOMOs differ for sp- or LMCT-transitions (Oldenburg & Vogler, 1996; Vogler & Nikol, 1992). Subsequent relaxation of the excited state is possible by emission or radiationless deactivation or by a bond cleavage under formation of a permanent photo-product (Nikol & Vogler, 1991). A precise assignment of the reactive excited state of $BiPh_3$ is difficult due to the high density of the energetic levels (Berger et al., 2012). Vogler and Nikol (1992) postulated a LMCT as the reactive excited state for $BiCl_3 \times C_6H_6$ eventually leading to Bi^0 and biphenyl. A comparable mechanism might be possible also for $BiPh_3$ where the LMCT causes formal one-electron reduction to Bi(II) and release of a $Ph^\bullet$ radical. In subsequent thermal reactions the Bi(II) species eventually yield Bi^0 whereas the phenyl radicals can react with the solvent or TMSC yielding benzene and/or substituted benzene derivatives. Indeed, we could detect benzene by GC–MS analyses and emission spectroscopy in a control experiment upon irradiation of $BiPh_3$ in ethanol.

While without any stabilizer the Bi atoms aggregate very fast to form large clusters and particles resulting in a grey precipitate, the addition of the TMSC allows for a controlled growth of the particles by providing nucleation sites at hydroxyl groups (0.45 per AGU) in the used TMSC derivative. Besides the nucleation sites, TMSC offers a rather high steric protection of nanoparticles due to its high molar weight, which prevents the particles from uncontrolled aggregation as well. In principle, it would be desirable to vary the DS_{Si} in these investigations to study the effect of the amount of hydroxyl groups in TMSC on the nanoparticle formation rate. However, although we have different samples available in our labs (DS 1.5 and DS 2.0 with similar DP), the insolubility of these materials in toluene does not allow to perform these experiments and the solvents capable of dissolving these derivatives and $BiPh_3$ (*i.e.* THF, $CHCl_3$) are not UV stable. The main byproducts, benzene and biphenyl, can be removed by lyophilization followed by exposure of the dry powder to high vacuum conditions (1×10^{-3} mbar) for several hours at room temperature. The size of the particles has been determined using transmission electron microscopy. In this way, monodisperse bismuth nanoparticles are obtained which are homogenously distributed inside the TMSC matrix.

Surprisingly, diffraction experiments clearly reveal the presence of amorphous bismuth nanoparticles, which is accompanied by diffuse scattering in electron diffraction experiments (Fig. 2).

To the best of our knowledge, this is the first report on the preparation of amorphous BiNPs up to date. Probably, the presence of a highly amorphous polymer (TMSC) prevents the particles from crystallization. Regarding potential applications (*e.g.* inkjet-printing) amorphous particles are favored over crystalline ones since the latter require higher melting points in order to obtain semi-metal films. Additionally, it is much easier to selectively convert the amorphous particles to the corresponding pure bismuth oxides phase, which could be advantageous in the design of new battery electrodes based on bismuth sodium titanate.

Here, it should be mentioned that the nanoparticles do not show any sign of agglomeration, even after 5 months of storage. TEM images clearly reveal the same size distribution as for "just-prepared" samples.

Since TMSC has been widely used as a precursor for the generation of biocompatible cellulosic materials (Aulin, Ahola, et al., 2009; Aulin, Yun, et al., 2009; Buchholz, Wegner, Stemme, & Odberg, 1996; Kargl et al., 2013; Kontturi, Thune, & Niemantsverdriet, 2003; Mohan et al., 2011, 2012; Orelma, Filpponen, Johansson, Laine, & Rojas, 2011), we were interested whether the silyl groups can be cleaved off in a similar way as in thin films for instance, where acidic vapors (*e.g.* HCl) are employed. In the ideal case, the BiNPs are not altered significantly, while the wettability of the matrix changes from hydrophobic to hydrophilic. After exposure of the grids containing the BiNPs in the TMSC matrix to acidic vapors of HCl, the films should shrink and all trimethylsilyl groups should leave the film. As expected, the matrix shrinks due to the conversion of TMSC to cellulose caused by the formation of hydrogen bonding, which leads to the formation of a porous structure on the grids concomitant with an increase in density (Kontturi & Lankinen, 2010) (TMSC: *ca.* 0.99 g cm^{-3}; cellulose: 1.5 g cm^{-3}). However, the BiNPs are still homogenously distributed within the cellulose matrix.

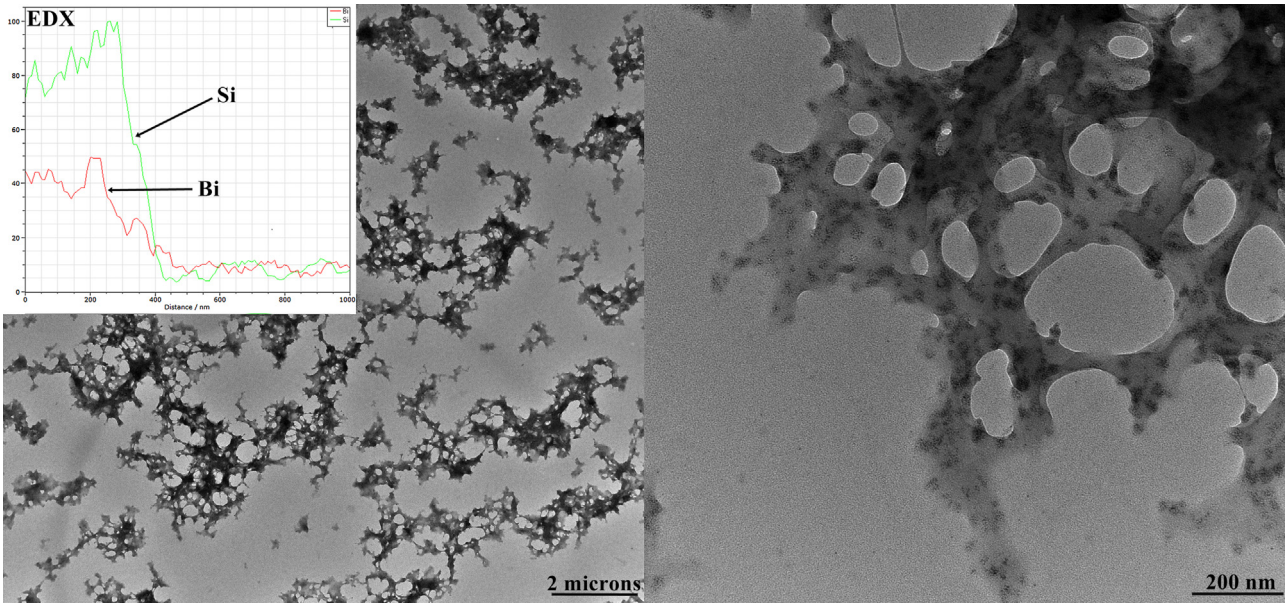

Fig. 3. TEM images of the BiNPs after exposure to HCl vapors for 15 min at different magnifications. An EDX line spectrum showing the presence of silicon and bismuth is incorporated in the left image.

Unexpectedly, the silyl groups do not leave the material but migrate from the TMSC matrix to the BiNPs which yields silylated BiNPs dispersed in a cellulose matrix. This can be explained by the formation of trimethylsilanol, Me_3SiOH, under the chosen reaction conditions, which is able to react with the thin oxide layer present on the outermost surface of the BiNPs. As proven with TEM/EDX, the local distribution of bismuth strongly correlates with the presence of silicon. TEM images after regeneration can be found in Fig. 3.

This *in-situ* trans-silylation procedure does not significantly affect the size of the particles (thickness of a TMS monolayer: *ca.* 0.5 nm) and although the silylation makes the particles hydrophobic, they remain homogenously distributed in the cellulose matrix as proven by HR-TEM. These images clearly show that TMS–BiNPs are not enriched at the air/polymer interface. Moreover, the contrast of the TMS–BiNPs in the TMSC matrix strongly varies, which can be related to their homogenous distribution inside the cellulose matrix. On first glance, the interaction between the cellulosic matrix and the silylated BiNPs must be repulsive since in many reports cellulose is considered to be mainly a hydrophilic polymer. However, recent progress on cellulose dissolution (Lindman, Karlström, & Stigsson, 2010; Medronho, Romano, Miguel, Stigsson, & Lindman, 2012) and also theoretical approaches (Bergenstrahle, Wohlert, Himmel, & Brady, 2010) in the field indicate that a much more differentiated view is required to understand the interaction behavior in cellulose (and its materials). In particular, hydrophobic interactions have been underestimated in this context. Although the proofs for the concept of amphiphilic cellulose, *i.e.* that cellulose has hydrophilic and hydrophobic interaction capacities, are rather strong, there is still an intense ongoing debate on this topic (Glasser et al., 2012). The silylated BiNPs do support the hypothesis that

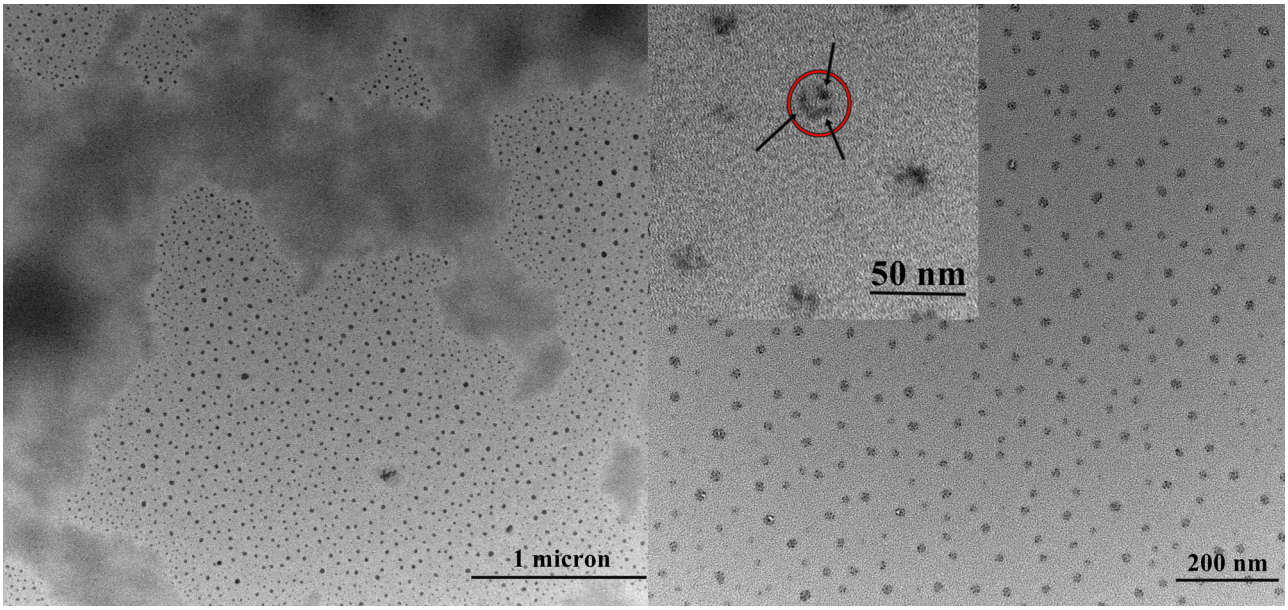

Fig. 4. TEM images after exposure of the grids to X-rays (EDX) for 15 min at different magnifications. Note the arrows which point at the three smaller nanoparticles composing the larger NPs.

cellulose is an amphiphilic polymer, because the shrinkage of the film should facilitate the removal of hydrophobic silylated nanoparticles from the cellulose matrix by phase separation. Indeed, we cannot observe such a phase separation. In contrast, our results do not indicate any sign of phase separation and the TMS–BiNPs are well distributed in the matrix, which probably can be attributed to hydrophobic interactions of cellulose with the TMS–BiNPs. In addition to these results, we observed an interesting feature of these TMS–BiNPs during EDX measurements. In the frame of the aforementioned experiments, we performed EDX experiments, whereby in the first series of measurements, the films have been exposed for a rather long time to the X-ray beam. There are some cases known where an increased energy input (*e.g.* by electron beams: electron beam fragmentation) induces structural and chemical changes, particularly in case of nanoparticles (Esmail, Bugayev, & Elsayed-Ali, 2013; Pyrz, Park, Vogt, & Buttrey, 2007). In a very recent example, BiNPs have been even synthesized by electron beam reduction from Bi_2O_3 (Weis, Schneider, Seipenbusch, & Kasper, 2013). In addition, the growth and decomposition (*i.e.* evaporation and coalescence) can be tuned by the properties of the electron beam. It turned out that during these EDX measurements the amount of bismuth in the matrix was decreasing over time and after 15 min the amount of bismuth was quite low. Obviously, under these conditions the BiNPs evaporate from the cellulose matrix and they can be found in the form of slightly smaller particles also outside the matrix (Fig. 4).

However, at a closer look using HR-TEM, it can be clearly seen that the particles have a different appearance as well and look more like aggregates of smaller particles than individual particles. It seems that the silyl groups prevent the particles from aggregation and coalescence to some extent.

4. Conclusion

In summary, an unconventional but highly reproducible synthesis for amorphous bismuth nanoparticles in a biopolymer matrix is described. For the proof of principle, easily accessible TMSC has been chosen as stabilizer but in principle any other polysaccharide can be used as well for this purpose as long as it exhibits sufficient photostability and solubility in the chosen solvent. The combination of polychromatic UV irradiation of solutions containing $BiPh_3$ and TMSC yields particles with a size of around 20 nm, which do not alter when the TMSC is converted to cellulose by HCl vapors. Future work will focus whether these particles can be used in inkjet printing of electrodes. However, for this purpose other silylethers of cellulose must be synthesized (*e.g. tert*-butyldimethylsilyl) and other solvent systems must be investigated since first preliminary attempts using this system (TMSC/toluene) were unsuccessful so far.

Acknowledgements

The research leading to these results has received funding from the People Programme (Marie Curie Actions – Career Integration Grants) of the European Union's Seventh Framework Programme (FP7/2007-2013) under REA grant agreement n°618158 and from the FP7-REGPOT Programme (CSA) under grant agreement n°264115.

References

Aulin, C., Ahola, S., Josefsson, P., Nishino, T., Hirose, Y., Österberg, M., et al. (2009). Nanoscale cellulose films with different crystallinities and mesostructures; their surface properties and interaction with water. *Langmuir*, *25*, 7675–7685.

Aulin, C., Yun, S. H., Wågberg, L., & Lindström, T. (2009). Design of highly oleophobic cellulose surfaces from structured silicon templates. *ACS Applied Materials & Interfaces*, *1*, 2443–2452.

Bergenstrahle, M., Wohlert, J., Himmel, M. E., & Brady, J. W. (2010). Simulation studies of the insolubility of cellulose. *Carbohydrate Research*, *345*, 2060–2066.

Berger, R. J. F., Rettenwander, D., Spirk, S., Wolf, C., Patzschke, M., Ertl, M., et al. (2012). Relativistic effects in triphenylbismuth and their consequences on molecular structure and spectroscopic properties. *Physical Chemistry Chemical Physics*, *14*, 15520–15524.

Briand, G. G., & Burford, N. (1999). Bismuth compounds and preparations with biological or medicinal relevance. *Chemical Reviews*, *99*, 2601–2657.

Buchholz, V., Wegner, G., Stemme, S., & Odberg, L. (1996). Regeneration, derivatization and utilization of cellulose in ultrathin films. *Advanced Materials*, *8*, 399–402.

Elschenbroich, C. (2005). *Organometallchemie*. Wiesbaden, Germany: Teubner Verlag.

Esmail, A. R., Bugayev, A., & Elsayed-Ali, H. E. (2013). Electron diffraction studies of structural dynamics of bismuth nanoparticles. *Journal of Physical Chemistry C*, *117*, 9035–9041.

Fischereder, A., Schenk, A., Rath, T., Haas, W., Delbos, S., Gougaud, C., et al. (2013). Solution-processed copper zinc tin sulfide thin films from metal xanthate precursors. *Monatshefte der Chemie – Chemical Monthly*, *144*, 273–283.

Glasser, W. G., Atalla, R. H., Blackwell, J., Malcolm Brown, R., Jr., Burchard, W., French, A. D., et al. (2012). About the structure of cellulose: Debating the Lindman hypothesis. *Cellulose*, *19*, 589–598.

Imran, M., Neumann, B., Stammler, H.-G., Monkowius, U., Ertl, M., & Mitzel, N. W. (2013). The versatile behaviour of a novel janus scorpionate ligand towards sodium, potassium and bismuth(III) ions. *Dalton Transactions*, *42*, 15785–15795.

Kargl, R., Mohan, T., Köstler, S., Spirk, S., Doliska, A., Stana-Kleinschek, K., et al. (2013). Functional patterning of biopolymer thin films using enzymes and lithographic methods. *Advanced Functional Materials*, *23*, 308–315.

Koehler, S., Liebert, T., & Heinze, T. (2008). Interactions of ionic liquids with polysaccharides. VI. Pure cellulose nanoparticles from trimethylsilyl cellulose synthesized in ionic liquids. *Journal of Polymer Science – Polymer Chemistry*, *46*, 4070–4080.

Kontturi, E., & Lankinen, A. (2010). Following the kinetics of a chemical reaction in ultrathin supported polymer films by reliable mass density determination with X-ray reflectivity. *Journal of the American Chemical Society*, *132*, 3678–3679.

Kontturi, E., Thune, P. C., & Niemantsverdriet, J. W. (2003). Cellulose model surfaces simplified preparation by spin coating and characterization by X-ray photoelectron spectroscopy, infrared spectroscopy, and atomic force microscopy. *Langmuir*, *19*, 5735–5741.

Kunkely, H., Paukner, A., & Vogler, A. (1989). Optical metal-to-ligand charge-transfer of 2,2′-bipyridyl complexes of antimony(III) and bismuth(III). *Polyhedron*, *8*, 2937–2939.

Lindman, B., Karlström, G., & Stigsson, L. (2010). On the mechanism of dissolution of cellulose. *Journal of Molecular Liquids*, *156*, 76–81.

Lusic, H., & Grinstaff, M. W. (2013). X-ray-computed tomography contrast agents. *Chemical Reviews*, *113*, 1641–1666.

Lutz, T., MacLachlan, A., Sudlow, A., Nelson, J., Hill, M. S., Molloy, K. C., et al. (2012). Thermal decomposition of solution processable metal xantahtes on mesoporous titanium dioxide films: a new route to quantum-dot sensitized heterojunctions. *Physical Chemistry Chemical Physics*, *14*, 16192–16196.

Medronho, B., Romano, A., Miguel, M. G., Stigsson, L., & Lindman, B. (2012). Rationalizing cellulose (in)solubility: Reviewing basic physicochemical aspects and role of hydrophobic interactions. *Cellulose*, *19*, 581–587.

Mohan, T., Kargl, R., Aleš Doliška Vesel, A., Kostler, S., Ribitsch, V., & Stana-Kleinschek, K. (2011). Wettability and surface composition of partly and fully regenerated cellulose thin films from trimethylsilyl cellulose. *Journal of Colloid and Interface Science*, *358*, 604–610.

Mohan, T., Spirk, S., Kargl, R., Doliska, A., Vesel, A., Salzmann, I., et al. (2012). Exploring the rearrangement of amorphous cellulose model thin films upon heat treatment. *Soft Matter*, *8*, 9807–9815.

Murakami, S. (2006). Quantum spin hall effect and enhanced magnetic response by spin-orbit coupling. *Physical Review Letters*, *97*, 236805.

Nikol, H., & Vogler, A. (1991). Photoluminescence of antimony(III) and bismuth(III) chloride complexes in solution. *Journal of the American Chemical Society*, *113*, 8988–8990.

Oldenburg, K., & Vogler, A. (1996). Photoredox chemistry of bismuth trichloride in benzene. *Journal of Organometallic Chemistry*, 515.

Oldenburg, K., Vogler, A., Mikó, I., & Horváth, O. (1996). Photoredox decomposition of tin(II), lead(II), antimony(III) and bismuth(III) iodide complexes in solution. *Inorganica Chimica Acta*, *248*, 107–110.

Orelma, H., Filpponen, I., Johansson, L.-S., Laine, J., & Rojas, O. J. (2011). Modification of cellulose films by adsorption of cmc and chitosan for controlled attachment of biomolecules. *Biomacromolecules*, *12*, 4311–4318.

Paez, R. M., & Hoggard, P. E. (2003). The photolysis of dichlorotriphenylbismuth(V) in chloroform. *Photochemical and Photobiological Sciences*, *2*, 142–144.

Pyrz, W. D., Park, S., Vogt, T., & Buttrey, D. J. (2007). Electron beam-induced fragmentation and dispersion of Bi–Ni nanoparticles. *Journal of Physical Chemistry C*, *111*, 10824–10828.

Reith, L. M., Stiftinger, M., Monkowius, U., Knoer, G., & Schoefberger, W. (2011). Synthesis and characterization of a stable Bi(III)A3 – Corrole. *Inorganic Chemistry*, *50*, 6788–6797.

Smith, G. E., Baraff, G. A., & Rowell, J. M. (1964). Effective *g* factor of electrons and holes in bismuth. *Physical Review*, *135*, A1118–A1124.

Tsang, C.-N., Ho, K.-S., Sun, H., & Chan, W.-T. (2011). Tracking bismuth antiulcer drug uptake in single helicobacter pylori cells. *Journal of the American Chemical Society*, *133*, 7355–7357.

Vogler, A., & Nikol, H. (1992). Photochemistry and photophysics of coordination compounds of the main group metals. *Pure & Applied Chemistry*, *64*, 1311–1317.

Wang, F., Tang, R., Yu, H., Gibbons, P. C., & Buhro, W. E. (2008). Size- and shape-controlled synthesis of bismuth nanoparticles. *Chemistry of Materials*, *20*, 3656–3662.

Warren, S. C., Jackson, A. C., Cater-Cyker, Z. D., DiSalvo, F. J., & Wiesner, U. (2007). Nanoparticle synthesis via the photochemical polythiol process. *Journal of the American Chemical Society*, *129*, 10072–10073.

Weis, F., Schneider, R., Seipenbusch, M., & Kasper, G. (2013). Synthesis of BI2O3/SIO2 core–shell nanoparticles by an atmospheric CVS/CVD process and their modification by hydrogen or electron-beam induced reduction. *Surface Coatings & Technology*, http://dx.doi.org/10.1016/j.bbr.2011.1003.1031 (in press)

Yarema, M., Kovalenko, M. V., Hesser, G., Talapin, D. V., & Heiss, W. (2011). Highly monodisperse bismuth nanoparticles and their three-dimensional superlattices. *Journal of the American Chemical Society*, *132*, 15158–15159.

Yu, S.-B., & Watson, A. D. (1999). Metal-based X-ray contrast media. *Chemical Reviews*, *99*, 2353–2377.